Synthesis of Octasubstituted Cyclooctatetraenes and Their Use as Electron Transporters in Organic Light Emitting Diodes

Ping Lu,[†] Haiping Hong, Guoping Cai,[‡] Peter Djurovich, William P. Weber,* and Mark E. Thompson*

Contribution from the Department of Chemistry and The Donald P. and Katherine B. Loker Hydrocarbon Research Institute, University of Southern California, Los Angeles, California 90089

Received January 31, 2000. Revised Manuscript Received April 17, 2000

Abstract: The synthesis and characterization of octasubstituted cyclooctatetraenes (COTs) as well as their use as electron transporting materials in organic LEDs are reported. Tetraaryl-tetraarylethynyl-cyclooctatetraenes [$C_8Ar_4(C{\equiv}CAr)_4$] were prepared from diaryldiynes with a $RuH_2(CO)(PPh_3)_3$ catalyst in good yield (40−80%). Octaaryl-cyclooctatraenes were prepared from diarylacetylenes by treatment with lithium and iodine in 50% yield. Cyclic voltametry indicates that these COTs are reduced in sequential one-electron steps. $C_8Ar_4(C{\equiv}CAr)_4$ and C_8Ar_8 are thermally stable to sublimation and have wide optical energy gaps [λ_{max}(emission) = 392−412 nm] making them good candidates for use in organic LEDs. These octasubstituted COTs have been used as electron transport layers in single heterostructure organic LEDs, i.e. ITO/NPD 400 Å/octasubstituted COT 400 Å/Mg−Ag (ITO = indium−tin oxide, NPD = *N*,*N*′-diphenyl-*N*,*N*′-dinaphthylbenzidine). External quantum efficiencies of 0.1−0.2% (photons/electrons) were observed, with turn-on voltages of ca. 6 V. The emission from this device comes exclusively from the NPD hole transporting layer, with a λ_{max} of 435 nm. Doping the NPD layer with 1% perylene leads to an increased quantum efficiency of 0.6% and an electroluminescence spectrum indicative of emission solely from the perylene dopant, confirming exclusive emission from the NPD hole transporting layer.

Introduction

Organic light-emitting devices (OLEDs) have received a great deal of attention recently, due to their promising applications in emissive displays.[1] OLEDs consist of a thin amorphous organic film or multilayer (ca. 1000 Å) sandwiched between anode and cathode contacts. The anode is typically a film of transparent indium tin oxide (ITO) precoated on a transparent substrate (e.g. glass) to allow for light emission and viewing. The different materials used in adjoining layers in an OLED consist of one that provides the predominant path for hole migration (the hole transporting layer, HTL) and a second that forms the path for electron migration (the electron transporting layer, ETL). When a voltage is applied across the two electrodes, carriers are injected into the organic film. As charged carriers migrate toward the opposite electrode (i.e. holes toward the cathode, electrons toward the anode) they recombine within the organic layer promoting one of the organic molecules into its excited state. Like the carriers, this excited state, or exciton, is mobile in the molecular thin film. The exciton migrates by diffusive hopping between adjacent molecules until it either radiatively or nonradiatively relaxes back to the ground state.[1−4]

A common technique used to tune the emission color in OLEDs is to use a low concentration (ca. 1 wt %) of an efficient fluorescent[5,6] or phosphorescent[7] dye, doped into the transport material to act as the emissive center. The dopant in this device traps the exciton and luminesces. In this way, the carrier conduction and emissive functions are decoupled. In dye-doped OLEDs, the emission color and efficiency can readily be tuned by modification of the dopant without affecting the electrical properties of the device.

A great deal of effort has been placed on developing new HTL materials for OLEDs.[1,8] The result has been a significant increase in the thermal stability and transporting properties of these materials. Comparatively less work has been reported on the development of new ETL materials. The most thoroughly studied electron transporting material in small molecule based

* To whom correspondence should be addressed. Weber: wpweber@usc.edu. Thompson: met@usc.edu.

[†] Permanent address: Department of Chemistry, Zhejiang University, Hangzhou, China

[‡] Permanent address: Department of Polymer Science & Engineering, Zhejiang University, Hangzhou, China

(1) Chen, C. H.; Shi, J.; Tang C. W. *Macrolmo/.Symp*. **1997**, *125*, 1. Forrest, S. R.; Burrows, P. E.; Thompson, M. E. *Laser Focus World* **1995**, *31*, (2), 99−107, Rothberg, L. J.; Lovinger, A. J. *J. Mater. Res*. **1996**, 11 (12), 3174−3187, Sibley, S.; Thompson, M. E.; Burrows, P. E.; Forrest, S. R. *Optoelectronic Properties of Inorganic Complexes;* Roundhill, D. M., Fakler, J., Eds.; Plenum Press: New York, 1998; Chapter 2.

(2) Powell, R. C.; Soos, Z. G. *J. Lumin.* **1975**, *11*, 1.

(3) Tang, C. W.; VanSlyke, S. A.; Chen, C. H. *J. Appl. Phys.* **1989**, *65*, 3610−3616.

(4) Burrows, P. E.; Shen, Z.; Bulovic, V.; McCarty, D. M.; Forrest, S. R.; Cronin, J.; Thompson, M. E. *J. Appl. Phys.*, **1996**, *79*, 7991.

(5) Shoustikov, A. A.; You, Y.; Thompson, M. E. *IEEE J. Selected Top.* **1998**, *4* (1), 3−13,

(6) Suzuki, H.; Hoshino, S. J. *Appl. Phys. Lett.* **1996,** *79*, 8816. Shoustikov, A.; You, Y.; Burrows, P. E.; Thompson, M. E.; Forrest, S. R. *Synth. Met.* **1997**, *91*, 217. Tang, C. W. *Dig. 1996 SID International Symposium,* SID: San Diego, CA, 1996; p 181. Wakimoto, T.; Yonemoto, Y.; Funaki, J.; Tsuchida, M.; Murayama, R.; Nakada, H.; Matsumoto, H.; Yamamura, S.; Nomura, M.; Tsutsui, T. *Synth. Met.* **1997**, *91*, 1−3, 15.

(7) Baldo, M. A.; O'Brien, D. F.; You, Y.; Shoustikov, A.; Sibley, S.; Thompson, M. E.; Forrest, S. R. *Nature* **1998**, *395*, 151. O'Brien, D. F.; Baldo, M. A.; Thompson, M. E.; Forrest, S. R. *Appl. Phys. Lett*, **1999**, *74*, 442. Baldo, M. A.; Lamansky, S.; Thompson, M. E.; Forrest, S. R. *Appl. Phys. Lett.* **1999**, *75*, 442. Kwong, R. C.; Sibley, S.; Baldo, M.; Forrest, S. R.; Thompson, M. E. *Chem. Mater.* **1999**, *11*, 3709.

10.1021/ja000354q CCC: $19.00
Published on Web 07/21/2000

OLEDs is aluminum tris(8-hydroxyquinoline), Alq_3.[1,9] Other metal complexes have been reported for use as ETL materials as well; however, their efficiencies and stabilities are typically worse than those of Alq_3-based OLEDs.[10] Heterocyclic compounds, such as oxidiazoles and triazolzes, have been the most thoroughly studied organic ETL materials.[11] ETL materials with large energy gaps are very desirable, since they could be used to fabricate OLEDs with a wide range of emission colors, including blue. Alq_3 and its analogues can be used for green to red OLEDs, but their energy gaps are too small to make them useful for blue OLEDs. While organic ETLs have been reported which can be used to fabricate blue OLEDs,[11,12] the efficiencies of these devices and their lifetimes are often poor. The goal of the work reported here is to develop new ETL materials, which can be used in blue OLEDs.

We have prepared a number of different octasubstituted cyclooctatetraenes (COTs) and investigated them as organic electron transporting materials in OLEDs. Previously reported synthetic routes to substituted COT derivatives typically give low yield.[14,18,15,22] In this paper we report novel, high-yield syntheses of both tetraaryl-tetraarylethynyl-COTs and octaaryl-COTs. These COTs form highly stable glasses and act as efficient electron transporting materials in organic LEDs. The energy gaps for the COT derivatives studied here are sufficiently wide (>3 eV) to make it possible to fabricate blue emitting OLEDs with these materials.

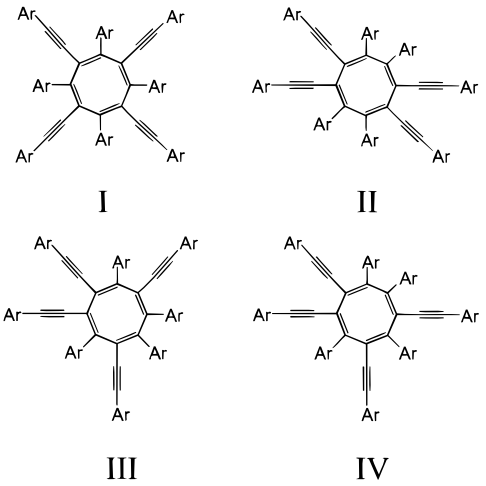

Figure 1. Possible structures of tetraaryl-tetraarylkynyl-cyclooctatetraene derivatives (Ar = arene). Acronyms used throughout the paper: Ar = phenyl (**COT-H**); Ar = *p*-tolyl (**COT-Me**); Ar = 2-thiophenyl (**COT-th**); Ar = *p*-anisole (**COT-OMe**).

Results and Discussion

Synthesis and Characterization of Octasubstituted Cyclooctatetraenes. Transition metal catalyzed cyclotrimerization of acetylenes to yield benzene derivatives is well-known.[13] On the other hand, the transition metal catalyzed cyclotetramerization of acetylenes to yield cyclooctatetraene derivatives is less common. Reppe reported that acetylene itself could be tetramerized by nickel catalysts to yield cyclooctatetraene (COT).[14] However, nickel catalysts do not work well for substituted acetylenes.[15]

We have previously reported that a ruthenium catalysts will copolymerize benzophenone and dialkynes.[16] When diphenylbutadiyne is treated with the Ru catalyst [$(Ph_3P)_3Ru(CO)H_2$ activated with a stoichiometric amount of styrene],[17] a cyclooctatetraene, **COT-H**, is formed. Ru-catalyzed cyclotetramerizations of di-*p*-tolylbutadiyne, di-*p*-methoxyphenylbutadiyne, and di(2-thienyl)butdiyne have also been carried out to produce the corresponding COT derivatives, abbreviated **COT-Me**, **COT-OMe**, and **COT-th**, respectively. This reaction is extremely efficient and selective. **COT-H** is formed in 86% yield after purification by chromatography and recrystallization. The molecular weight of the tetramer was established by mass spectrometry. The major fragmentation pathway of the parent cation radical is loss of diphenylbutadiyne to give a trimer cation radical. Most of the octasubstituted COTs form stable glasses, with high glass transition temperatures, e.g., T_g values for **COT-H**, **COT-Me**, and **COT-OMe** are 177, 214, and 194 °C, respectively. They are thermally stable and do not undergo loss of weight by TGA below 310 °C.

Assuming the aryl groups and the other carbons of the starting diphenylbutadiyne maintain their initial connectivity, there are four possible isomeric cyclooctatetraenes which can be formed, labeled I−IV in Figure 1. Cyclooctatetraenes are not planar but instead have been shown to be tub-shaped molecules, which are highly fluxional at room temperature.[18,19] On the basis of a tub conformation for the COT ring (ignoring the phenyl ring conformations), I and II each have D_2 symmetry, III has C_2 symmetry, while isomer IV has C_1 symmetry. Therefore, the number of acetylenic resonances in the ^{13}C NMR for each isomer is expected to be two, two, four, and eight for isomers I, II, III, and IV, respectively. In fact, the ^{13}C NMR spectra of **COT-H** has eight distinct acetylenic carbon resonances. This is consistent with the unsymmetrical isomer IV. Similarly, eight

(8) (a) O'Brien, D. F.; Burrows, P. E.; Forrest, S. R.; Koene, B. E.; Loy, D. E.; Thompson, M. E. *Adv. Mater.* **1998**, *10*, 1108. (b) Koene, B. E.; Loy, D. E.; Thompson, M. E. *Chem. Mater.* **1998**, *10*, 2235. (c) Adachi, C.; Tsutsui, T.; Saito, S. *Optoelectron. Dev. Technol.* **1991**, *6*, 25. (d) VanSlyke, S. A.; Chen, C. H.; Tang, C. W. *Appl. Phys. Lett.* **1996**, *69*, 2160. (e) Shirota, Y. *J. Mater. Chem.* **2000**, *10*, 1.

(9) Schmidt, M. L.; Anderson, N. R.; Armstrong, *J. Appl. Phys.* **1995**, *78*, 5619. Saito, S.; Tsutsui, T.; Era, M.; Takada, N.; Adachi, C.; Hamada, Y.; Wakimoto, T. *Proc. SPIE* **1993**, *1910*, 212. Tang, C. W.; VanSlyke, S. A.; Chen, C. H. *J. Appl. Phys.* **1989**, *65*, 3610. Curioni, A.; Andreoni, W. *J. Am. Chem. Soc.* **1999**, *121*, 8216.

(10) Kido, J.; Hayase, H.; Hongawa, K.; Nagai, K.; Okuyama, K. *Appl. Phys. Lett.* **1994**, *65*, 2124. Kawamura, Y.; Wada, Y.; Hasegawa, Y.; Iwamuro, M.; Kitamura, T.; Yanagida, S. *Appl. Phys. Lett.* **1999,** *74*, 3245. Gao, X. C.; Cao, H.; Huang, C. H.; Li, B. G.; Umitani, S. *Appl. Phys. Lett.* **1998,** *72*, 2217.

(11) Hamada, Y.; Adachi, C.; Tsutsui, T.; Saito, S. *Jpn. J. Appl. Phys.* **1992**, *31*, 1812. Kido, J.; Ohtaki, C.; Hongawa, K.; Okuyama, K.; Nagai, K. *Jpn. J. Appl. Phys.* **1993**, *32*, 917. Antoniadis, H.; Inbasekaran, M.; Woo, E. P. *Appl. Phys. Lett.* **1998**, *73*, 3055.

(12) Kijima, Y. Materials Research Society Abstracts, Spring Meeting, San Francisco, 1998. Nakada, H.; Kawami, S.; Nagayama, N.; Yonemoto, Y.; Muayama, R.; Funaki, J.; Wakimoto, T.; Imai, K. *Polym. Prepr. Jpn.* **1994**, *43*, 2450.

(13) Berthelot, M. *Ann.* **1866,** *139*, 273.

(14) (a) Reppe, W.; Schweckendiek, W. J. *Ann.* **1948,** *560***,** 104. (b) Schröder, G. *Cyclooctatetraenes*; Verlag-Chemie: Weinheim, Germany, 1965.

(15) Leto, J. R.; Leto, M. F. *J. Am. Chem. Soc.* **1961,** *83*, 2944.

(16) Lonergan, T. M.; You, Y.; Thompson, M. E.; Weber, W. P. *Macromolecules* **1998**, *31*, 2784.

(17) Guo, H.; Wang, G.; Tapsak, M. A.; Weber, W. P. *Macromolecules* **1995,** *28*, 5686.

(18) Lowry, T. H.; Richardson, K.; Schueller *Mechanism and Theory in Organic Chemistry*; Harper and Row: New York, 1976.

(19) Anet, F. A. L.; Bourn, A. J. R.; Lin, Y. S. *J. Am. Chem. Soc.* **1964,** *86*, 3576.

(20) Freedman, H. H. *J. Am. Chem. Soc.* **1961**, *83*, 2195.

(21) Huang, L.; Aulwurn, U. R.; Heinemann, F. W.; Kisch, H. *Eur. J. Inorg. Chem.* **1998**, 1951.

(22) (a) Braye, E. H.; Hubel, W. *J. Am. Chem. Soc.* **1961**, *86*, 4725. (b) Hoberg, H.; Frolich, C. *Angew. Chem.* **1980**, *92*, 131. (c) Frolich, C.; Hoberg, H. *J. Organomet. Chem.* **1981**, *201*, 131. (d) Eisch, J. J.; Piotrowski, A. M.; Systems, N. *Z. Naturforsch. B, Anorg. Chem., Org. Chem.* **1985**, *40B*, 624. (e) Hoberg, H.; Richter, W. *J. Organomet. Chem.* **1980**, *195*, 355. (f) Hoberg, H.; Richter, W. *J. Organomet. Chem.* **1980**, *195*, 347. (g) Eisch, J. J.; Galle, J. E.; Aradi, A. A.; Beleslawski, M. P. **1986**, *312*, 399. (h) Calderazzo, F.; Marchetti, F.; Pampaloni, G.; Hiller, W.; Antropiusova, H.; Mach, K. *Chem. Ber.* **1989**, *122*, 2229.

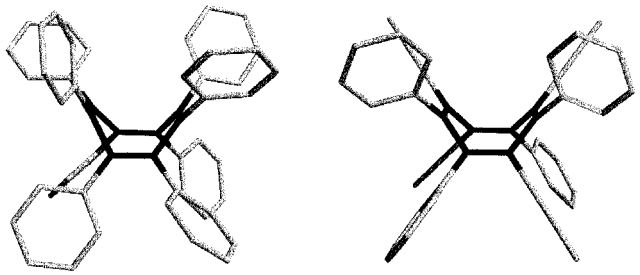

Figure 2. Molecular models of C_8Ph_8 (left) and $C_8Ph_4(C{\equiv}CMe)_4$ (right) determined at the PM3 level of theory. The structure of C_8Ph_8 determined here is very similar to that reported from crystallographic studies.[23]

resonances due to acetylenic carbons are seen in the ^{13}C NMR of **COT-Me** and **COT-OMe**. The ^1H NMR of **COT-Me** and **COT-OMe** are also consistent with isomer IV. Seven resonances for the methyl (or methoxy) groups are observed with six of these of equal intensity while one has an intensity that is twice as large. Apparently, two of the methyl groups and two of the methoxy groups fortuitously have identical chemical shifts. Thus, the unsymmetrical cyclooctatetraene IV appears to be the sole isomeric product of the ruthenium-catalyzed cyclotetramerization of diphenylbutadiyne. Interestingly, treatment of methyl propiolate with a tetrakis(phosphorus trihalide)-nickel(0) complex also gave 1,2,4-tricarbomethoxybenzene and the unsymmetrical 1,2,4,6-tetracarboethoxycyclooctadetraene as the sole products.[15] The reason for the regioselectively observed, which favors the unsymmetrical COT, is not understood.

Octaaryl-COTs, octaphenylcyclooctatetraene and tetraphenyl-tetra(*m*-tolyl)-cyclooctatetraene, $C_8Ph_4(m\text{-tol})_4$, were also prepared to study the influence of the alkynyl groups on the electronic properties of tetraaryl-tetraaryethynyl-COTs. Unfortunately, treatment of diphenylacetylene with the ruthenium catalyst does not yield C_8Ph_8,[20] but rather 1,2,3-triphenylnaphthene.[21] C_8Ph_8 has been prepared by a number of different routes.[20,22] Two of these routes involve dilithio-1,2,3,4-tetraphenyl-1,3-butadiene, which is first converted to an organometallic[20] or halogenated[22a] compound, and pyrolyzed to give C_8Ph_8. Our synthesis of octaaryl-COTs goes through the dilithiobutadiene as well, but couples it in situ to give the desired COT, in a "one pot" synthesis. Thus treatment of diphenylacetylene with lithium metal in diethyl ether, yields a dark red-brown solution of dilithio-1,2,3,4-tetraphenyl-1,3-butadiene. Addition of a solution of iodine in diethyl ether generates the diiodobutadiene derivative in situ, which couples efficiently with the dilithio reagent to give C_8Ph_8, in ≈50% yield. Tetraphenyl-tetra(*m*-tolyl)-cyclooctatetraene was prepared in a similar manner from phenyl-*m*-tolyl-acetylene, and isolated in >50% yield.

While it has not been possible to get X-ray crystallographic quality crystals of the tetraaryl-tetraarylethynyl-COT derivatives, we assume that they are structurally similar to the octaphenyl derivatives. The X-ray crystal structure of C_8Ph_8 has been reported and has a tub conformation for the COT core.[23] The COT core shows bond alternation between single (1.51 Å average) and double (1.35 Å average) bonds with 120° bond angles at each carbon in the ring. The phenyl rings are all bound at normal single bond lengths (average = 1.50 Å), and oriented to minimize inter-aryl repulsions. Molecular modeling of both C_8Ph_8 and $C_8Ph_4(C{\equiv}CMe)_4$ minimize to structures with a COT core in a tub conformation (Figure 2). The tetraaryl-tetraalkynyl-COT has a structure very similar to that of the octaphenyl derivative, with aryl and alkynyl groups twisted to minimize contacts as seen in C_8Ph_8. C_8Ph_8 and $C_8Ph_4(C{\equiv}CMe)_4$ have both their HOMO and LUMO levels localized on the C_8 core.

Electronic Properties of COT Derivatives. All of the tetraaryl-tetraarylethynyl-COTs prepared here show strong absorption bands in the ultraviolet and fluorescence in the violet part of the spectrum (Table 1). The fluorescence λ_{max} values fall between 392 and 412 nm, and all have full width and half-maximum values of 50−60 nm (ca. 3500 cm^{-1}). The excitation spectra of all of the COT derivatives show maximum intensities near the fluorescence maximum, e.g. Figure 3. The small Stokes shift between the excitation or absorption and emission is consistent with the high fluorescence quantum yields from these materials. **COT-Me** and **COT-OMe** have the highest fluorescent quantum yields of 0.5 and 0.8, respectively.

The absorption spectra of these materials display their λ_{max} values at significantly higher energies than their excitation maxima. There is an intense band near the fluorescence peak, but the dominant absorption is deeper in the UV. The intensity and energy of this higher energy UV absorption band is strongly affected by the aryl group substitution, while the lower energy band near the fluorescence peak is only weakly perturbed. The higher energy band most likely involves excitation into one of the higher energy π^* states, S_n ($n > 1$), largely localized on the arenes, rather than the direct promotion to the lowest energy excited state, S_1. In calculating the optical gap for these materials, the lower energy absorption band was used, which correlates well with the excitation spectrum. The optical gap for each compound, Table 1, was estimated by the point of intersection of the normalized absorption and emission bands.

Considering the variety of arenes used here, it is surprising that the range of emission energies and optical gaps is so small. The principal reason for the low sensitivity of the electronic transition energies to the arene substituent is that the lowest energy transitions are localized in the π system of the COT core. For steric reasons, the arenes bound directly to the COT core are not conjugated to the COT while the arylethynyl groups show very poor conjugation, even though the π overlap can be significant. As a result, the substituent effects are not well communicated to the COT core. This conclusion is supported by the molecular orbital calculations discussed above as well as the photophysical properties of octaaryl-COT compounds. The fluorescence energies and optical gaps for C_8Ph_8 and $C_8Ph_4(m\text{-tol})_4$ are very similar to those of the tetraphenyl-tetraarylethynyl derivatives, consistent with the lowest energy transition being localized on the C_8 core (Table 1), and not involving the arylethynyl groups.

Three of the COT derivatives reported here show reversible reductions in DMF solvent between −1.5 and −1.8 V relative to $Ag^+/AgCl$, Table 1. The other materials show solvent reduction only. Oxidation waves are not observed for any of these materials. Integration of the COT reduction wave relative to an internal ferrocene reference shows that the wave corresponds to a one-electron reduction of the COT. One-electron reduction waves are also observed for other COT derivatives. C_8H_8 as well as alkyl-COT derivatives give two separate waves for the $0/1^-$ and $1^-/2^-$ couples.[24−26] For example, the first and second reduction potentials for C_8H_8 fall at −1.62 and −1.86 V in DMF. In contrast, 1,3,5,7- and 1,2,4,7-tetraphenylcyclooc-

(23) Pawley, G. S.; Lipscomb, W. N.; Freeman, H. H. *J. Am. Chem. Soc.* **1964**, *86*, 4725. Wheatley, P. J. *J. Chem. Soc.* **1965**, 3136.

(24) Allendoerfer, R. D.; Reiger, P. H. *J. Am. Chem. Soc.* **1965**, *87*, 2336.

(25) Dewar, M. J. S.; Harget, A.; Haselbach, E. *J. Am. Chem. Soc.* **1969**, *91*, 168. Allinger, N. L.; Sprague, J. T.; Finder, C. J. *Tetrahedron* **1973**, *29*, 2519.

(26) Paquette, L. A.; Ley, S. V.; Meisinger, R. H.; Russell, R. K.; Oku, M. *J. Am. Chem. Soc.* **1974**, *96*, 5806.

Table 1. Spectroscopic and Electrochemical Data for Cyclooctatetraene Derivatives

groups bound to cyclooctatetraene	acronym	absorption λ_{max} (nm)	photoluminescence λ_{max} (nm)	ϕ (quantum yield)	energy gap (eV)	$E_{1/2}$ (DMF, V vs $Ag^+/AgCl$)[a]	$E_{1/2}$ (MeCN, V vs $Ag^+/AgCl$)[a]
$Ph_4(C{\equiv}CPh)_4$	COT-H	313, 364	392	0.2	3.3	−1.68	−1.64
$(p\text{-tolyl})_4(C{\equiv}C\text{-}p\text{-tolyl})_4$	COT-Me	318, 367	402	0.5	3.25	−1.59	−1.58
$(2\text{-thiophene})_4(C{\equiv}C\text{-}2\text{-thiophene})_4$	COT-th	317, 365	410	0.06	3.25	−1.71	
$(p\text{-anisolyl})_4(C{\equiv}C\text{-}p\text{-anisolyl})_4$	COT-OMe	318, 364	412	0.8	3.2		
Ph_8	C_8Ph_8	277	392	solubility low	3.3		−1.62
$Ph_4(m\text{-tolyl})_4$	$C_8Ph_4(m\text{-tol})_4$	266	402	0.2	3.3		

[a] If a value is not listed, only solvent reduction is observed, due to either low solubility of the COT derivative or the reduction potential for that derivative falling at a more negative potential than solvent reduction. When ferrocene is added to the cell, its oxidation wave is seen at +0.5 V vs $Ag^+/AgCl$.

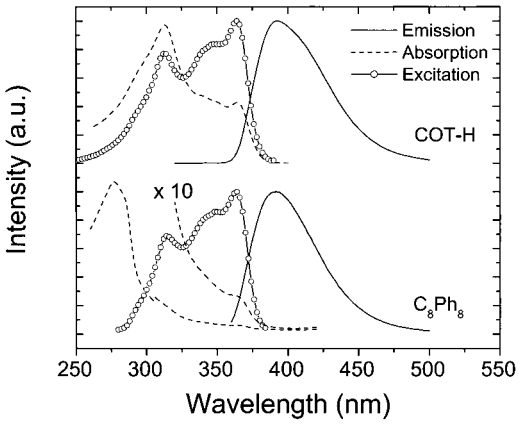

Figure 3. Absorption, emission, and excitation spectra of **COT-H** and C_8Ph_8 in CH_2Cl_2 solution.

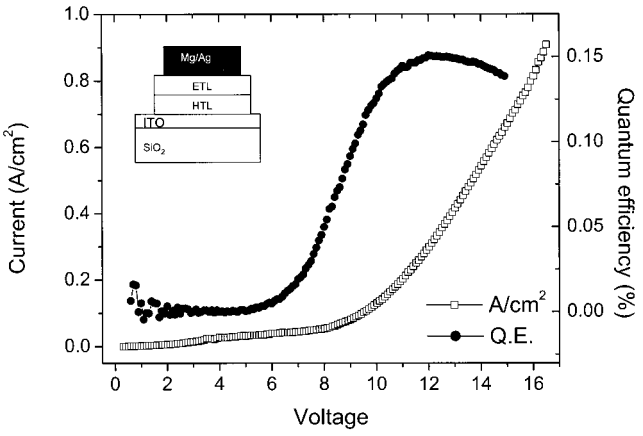

Figure 4. Current−voltage and efficiency−voltage plots for an OLED utilizing a **COT-Me** ETL (ITO/400 Å NPD/400 Å **COT-Me**/Mg−Ag). The inset shows a schematic representation of the OLEDs prepared here.

tatetraenes show a single two-electron reduction in acetonitrile.[27] Both of these tetraphenyl derivatives are expected to have a more stable COT dianion than C_8H_8 or its alkyl-substituted derivatives, due to delocalization of the negative charges onto the phenyl groups, shifting the second reduction anodic of the first. Severe steric interactions between adjacent groups prevent the aryl groups of the octasubstituted-COT derivatives from becoming coplanar with the COT core. Thus, we expect the electrochemistry of these octasubstituted COTs to show two sequential one-electron reductions, similar to the situation observed for C_8H_8 and its alkyl-substituted derivatives. In fact, the steric constraints of the octasubstituted COT ring apparently destabilize the planar COT form so much that we do not observe the second reduction wave in the potential range available in DMF (our lower limit in DMF was −2.2 V).

Organic LEDs Utilizing COT Derivatives. There are a number of important properties an efficient carrier transporting or emissive layer in OLEDs must possess. The material must be stable toward sublimation and form a stable glassy film. Recrystallization of the thin film in an OLED will lead to decreased device efficiency. The COT derivatives prepared here all have good thermal stability toward sublimation and have high glass transition temperatures. If the material is to act as both a carrier transporting and emitting layer it is important for the compound to luminesce efficiently in the solid state. The quantum yields for fluorescence reported in Table 1 were determined in fluid solution, so they do not bear directly on the solid state luminescence efficiencies. While we have not attempted to determine the quantum efficiencies for these materials in the solid state, they are strongly emissive in either powdered or thin film form. The measured reduction potentials for the octasubstituted COT derivatives (between −2.1 and −2.3, relative to ferrocene/ferrocenium) are similar to that of the common electron transporter, Alq_3 (−2.30 V relative to the same reference).[28] Thus, we expect that the LUMO levels of the COTs should be close to the energy of Alq_3, but that the HOMO levels of the COTs should be below those of Alq_3, due the larger energy gap for the COTs, relative to Alq_3.

To test the usefulness of COT derivatives in OLEDs as carrier transporting or emitting materials, we have prepared a number of single heterostructure OLEDs. These devices were prepared on indium−tin oxide (ITO) coated glass slides by vacuum depositing a 400 Å HTL (NPD or COT derivative), a 400 Å ETL (Alq_3 or COT derivative), and a 600 Å cathode composed of 10:1 Mg−Ag. The ITO anodes were patterned prior to deposition to define the devices. The organic and metal films deposited sequentially, without breaking vacuum throughout the deposition process. The devices were tested in the air within 1 h of removing them from high vacuum. No changes were observed in device properties for at least 3 h under these conditions.

Efficient blue electroluminescence is observed when **COT-Me** is used as an ETL in a standard OLED (ITO/NPD/**COT-Me**/Mg−Ag). The current−voltage and efficiency−voltage plots are shown in Figure 4. The current−voltage curves are typical for OLEDs with a turn-on voltage (the point where the quantum efficiency steeply rises from 0) for this device of roughly 7 V. The emission spectrum from this device is centered at 435 nm, consistent with exclusive emission from the NPD layer in this

(27) Rieke, R. D.; Copenhafer, R. A. *Tetrahedron Lett.* **1971**, *44*, 4097−4100.

(28) Anderson, J. D.; McDonald, E. M.; Lee, P. A.; Anderson, M. L.; Ritchie, E. L.; Hall, H. K.; Hopkins, T.; Mash, E. A.; Wang, J.; Padias, A.; Thayumanavan, S.; Barlow, S.; Marder, S. R.; Jabbour, G. E.; Shaheen, S.; Kippelen, B.; Peyghambarian, N.; Wightman, R. M. *J. Am. Chem. Soc.* **1998**, *120*, 9646.

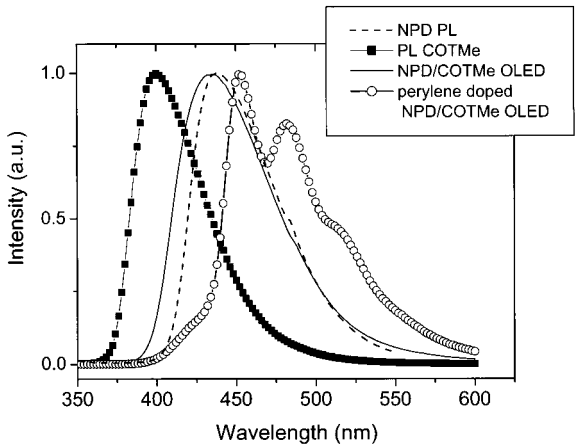

Figure 5. Photoluminescence spectra of **COT-Me** and NPD, as well as the electroluminescence spectra of the **COT-Me**-based OLED (ITO/NPD/**COT-Me**/Mg−Ag) and the perylene-doped OLED (ITO/NPD·perylene/**COT-Me**/Mg−Ag).

device. The photoluminescence spectra of NPD and **COT-Me** are shown along with the electroluminescence spectra of the **COT-Me** device in Figure 5. The energy gap for NPD is lower than that of COT, so it is not surprising that the emission appears to be from the NPD layer. The maximum efficiencies for this device are 0.16% (0.1 lum/W). The efficiency values in lum/W for this device are lower than might be expected for the observed quantum efficiency; however, it is important to take into account the fact that the bulk of the emission band for this device is on the tail of the photopic response function, leading to low luminance values.[5] A low luminance efficiency does not prevent this device from having a reasonable brightness. The maximum luminance observed for this device was 280 Cd/m^2 at 18 V.

Transporting electrons in the **COT-Me**-based OLED could be done by formation and migration of either anion-radical or dianionic carriers in the **COT-Me** film. The charge in either case would hop from **COT-Me** to **COT-Me** until it either reached the HTL/ETL interface or recombined with hole to form an exciton within the **COT-Me** layer. While both carriers are theoretically possible, the anion-radical is most likely the carrier in these materials. The dianionic forms of COTs are aromatic and thus are expected to have good stability, but they are not expected to be stable in a neutral nonpolar medium such as neat **COT-Me** or other octasubstituted COTs. Without countercations to form tight ion pairs or transition metal ions to complex the COT^{2-}, the dianion rapidly reduces a neutral COT, leading to two monoanionic COTs.[29]

While the majority of the emission is clearly coming from the HTL layer in the NPD/**COT-Me** OLED, the emission bands for the two materials overlap and there may be some contribution from the **COT-Me** layer. To determine if the emission from the NPD/**COT-Me** OLED was coming exclusively from the NPD layer, an OLED was prepared with a perylene dopant (1 wt %) in the NPD layer. The perylene absorption band overlaps very well with the NPD emission band, leading to very efficient energy transfer/trapping of the NPD exciton to perylene.[5] The resulting emission spectrum will be that of perylene, rather than NPD. The perylene spectrum is red-shifted relative to NPD and shows distinctive vibronic fine structure, such that any emission from **COT-Me** would be clearly visible in the spectra. Figure 5 shows the spectrum of the perylene doped OLED (ITO/400 Å NPD·perylene/400 Å **COT-Me**/Mg−Ag). The electroluminescence spectrum is that of the perylene dopant, with a small shoulder at 435 nm from residual NPD emission. There is no band present at the λ_{max} for **COT-Me** (410 nm), consistent with emission only from the HTL. To confirm this effect, a device was prepared in which perylene was doped into the **COT-Me** layer (ITO/NPD/**COT-Me**·perylene/Mg−Ag). The electroluminescence spectra of this device is identical with that of the undoped device, i.e. $\lambda_{max} = 435$ nm, again consistent with only NPD emission.

In addition to establishing the site of emission in these **COT-Me**-based devices the perylene dopant increases the quantum efficiencies of the doped devices significantly. The perylene-doped device gives an external quantum efficiency of 0.6% and a luminance efficiency of 0.24 lum/W. The quantum and luminance efficiencies for this device are comparable to other blue emitting OLEDs.[8e,30] The luminance efficiency is increased because of the increased quantum efficiency as well as the red shift in the emission spectrum. The peak brightness for this device is 750 Cd/m^2 at 20 V.

Changing the layer thicknesses in an OLED can significantly affect the current−voltage characteristics as well as the efficiency of the device. To investigate the effect of the thickness of the **COT-Me** layer on device performance, an OLED was prepared with a 200 Å thick layer of **COT-Me** (ITO/400 Å NPD/200 Å **COT-Me**/Mg−Ag). As seen before, the emission from this device comes exclusively from the NPD layer. The current−voltage curve and turn-on voltage both shift to lower potentials by ca. 2−3 V. The shift is consistent with a significant amount of the electric field being dropped over the **COT-Me** layer only, rather than over the entire thickness of the organic film. The same phenomena is observed for other OLEDs (e.g. NPD/Alq_3 devices[31]). Unfortunately, in addition to lowering the turn-on voltage, thinning the **COT-Me** layer also leads to a significant drop in the quantum efficiency to 0.06%. The decreased efficiency is most likely due to either carrier or exciton leakage through the thinner **COT-Me** film.

All of the data present thus far involve the use of **COT-Me** as an ETL. When the COT derivative is used as an HTL (ITO/**COT-Me**/Alq_3/Mg−Ag) the device gives only weak emission from Alq_3 (external quantum yield $< 10^{-3}$ %) and the current−voltage curves are shifted to substantially higher potential than that of the device where **COT-Me** is used as an ETL (shift = ca. 20 V). Clearly, the **COT-Me** layer does not act as a useful HTL in OLEDs utilizing the standard Alq_3 ETL.

OLEDs have also been fabricated with **COT-H** as an ETL. These devices were analogues of the **COT-Me** devices with 400 Å **COT-H** ETL layers (i.e. ITO/400 Å NPD/400 Å **COT-H**/Mg−Ag). The energy gap as well as the LUMO and HOMO energies for the two COT derivatives are very similar, Table 1. Both devices give emission exclusively from the NPD layer and display similar current−voltage plots. However, the **COT-H** curve is shifted to higher voltage by roughly 4 V, and the turn-on voltage increased to 10 V, compared to 7 V for **COT-Me**. The external quantum efficiency for the **COT-H** device is only 0.06%, relative to the 0.16% observed for the **COT-Me**-based

(29) Katz, T. J. *J. Am. Chem. Soc.* **1960**, *85*, 2360. Paquette, L. A.; Hansen, J. F.; Kakihana *J. Am. Chem. Soc.* **1971**, *93*, 168.

(30) Grice, A. W.; Bradley, D. D. C.; Bernius, M. T.; Inbasekaran, M.; Wu, W. W.; Woo, E. P. *Appl. Phys. Lett.* **1998**, *73*, 629. Hosowaka, C.; Kawasaki, N.; Sakamoto, S.; Kusumoto, T. *Appl. Phys. Lett.* **1992**, *61*, 2503. Wu, C. C.; Sturm, J. C.; Register, R. A.; Tian, J.; Dana, E. P.; Thompson, M. E. *IEEE Trans. Electron Dev.* **1997**,*44*, 1269. Pei, Q.; Yang, Y. *Adv. Mater.* **1995**, *7*, 559. Gao, Z.; Lee, C. S.; Bello, I.; Lee, S. T.; Chen, R.; Luh, T.; Shi, J.; Tang, C. W. *Appl. Phys Lett.* **1999**, *74*, 865. Noda, T.; Ogawa, H.; Shirota, Y. *Adv. Mater.* **1999**, *11*, 283. Hamada, Y.; Adachi, C.; Tsutsui, T.; Saito, S. *Jpn. J. Appl. Phys.* **1992**, *31*, 1812.

(31) Burrows, P. E.; Shen, Z.; Bulovic, V.; McCarty, D. M.; Forrest, S. R.; Cronin, J.; Thompson, M. E. *J. Appl. Phys.* **1996**, *79*, 7991−8006.

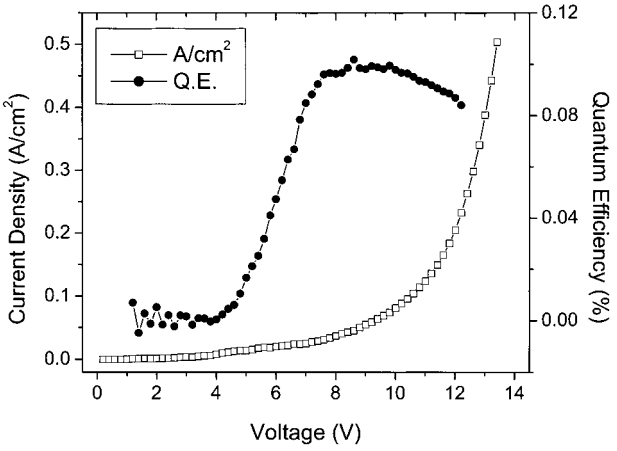

Figure 6. Current−voltage and efficiency−voltage plots for an OLED utilizing a C_8Ph_8 ETL (ITO/400 Å NPD/400 Å C_8Ph_8/Mg−Ag).

device. Several OLEDs were made with each material and consistently gave similar results to those described above. It is interesting that the OLEDS made with **COT-H** and **COT-Me** behave so differently, considering the similarity in their electrochemical and optical properties.

The electronic structure and electron transporting properties of the $C_8Ar_4(C{\equiv}CAr)_4$ derivatives may be influenced by the interactions between the arylethynyl groups and the central cyclooctatetraene core. To see if the arylethynyl groups contribute to the electron transporting properties of the COTs, we have prepared and investigated octaarylcyclooctatetraenes. C_8Ph_8 forms a stable glass, with a T_g of 110 °C. OLEDs were prepared with the C_8Ph_8 as the electron transporting layer, i.e. ITO/400 Å NPD/400 Å C_8Ph_8/Mg−Ag. Just as in the previous devices, the electroluminescence comes from the NPD layer (λ_{max} = 435 nm). The current−voltage curve for this device is very similar to that of the **COT-Me** OLED; however, the turn-on voltage of this device is roughly 5 V, Figure 6. The quantum efficiency of the C_8Ph_8-based OLED is 0.12%. The fact that this octaaryl-COT derivative performs as well as the tetraaryl-tetraarylethynyl-COTs strongly suggests that the COT core is intimately involved in the electron-transfer properties of these materials. The aryl groups are, however, very important to both inhibit crystallizations, hinder planarization of the COT core on reduction, and may be involved in intramolecular electron transfer (carrier migration).

Conclusion

We have demonstrated that octasubstituted cyclooctatetraenes can be made in high yield from either diaryldiynes of diarylalkynes. The high degree of substitution in the COT derivatives reported here keeps them stable and helps prevent crystallization. These materials have wide energy gaps, with strong fluorescence in the violet to ultraviolet part of the spectrum. The wide energy gaps of these materials are beneficial in making blue LEDs, since the COTs have an energy gap large enough to efficiently contain the emitting exciton within the organic film, preventing diffusion to the cathode, where it would be nonradiatively quenched. This is evident in the OLEDs presented here. In single heterostructure devices, i.e. ITO/NPD/COT/Mg−Ag, the emission comes exclusively from the NPD layer, either doped or undoped. The efficiencies of these devices are similar to other OLEDs which emit from an NPD layer, showing that the COT acts as an efficient electron transporting material.

The OLED structures used here are simple two-layer devices. In this two-layer structure, the COT layer transports electrons to the NPD/COT interface and prevents the leakage of holes from the NPD layer to the cathode. Considering the wide energy gap in these materials, they may also make excellent candidates for exciton confining or blocking layers. Devices incorporating such blocking layers have been used to make highly efficient phosphorescence-based OLEDs as well as efficient blue OLEDs.[32] These devices have the following structure: anode/HTL/blocking-layer/ETL/cathode. To be a useful blocking layer, the COT would need to transport electrons and block holes or excitons from diffusing to the ETL. The properties demonstrated for COT-based ETLs suggest that they may also make good blocking layers in such heterostructure devices. The use of COT derivatives as blocking layers is currently being investigated and will be reported in a future publication.

Experimental Section

Synthesis. Cuprous chloride, cuprous iodide, 2,7-dimethyl-3,5-octadiyne-2,7-diol, diphenylbutadiyne, *p*-bromoanisole, phenylacetylene, *p*-tolylacetylene, trimethylsilylacetylene, bis(triphenylphosphine)palladium dichloride, and tetrakis(triphenylphosphine)palladium, were purchased from Aldrich and used as received. Dihydridocarbonyltris-(triphenylphosphine)ruthenium[33] was prepared from ruthenium trichloride hydrate (Aldrich). All reactions were run in flame-dried glassware. Syntheses of the starting Ar−C≡CC≡C−Ar and Ar−C≡C−Ar compounds are given in the Supporting Information.

Spectroscopy, Analysis, and Thermal Measurements. ^{1}H and ^{13}C NMR spectra were obtained in $CDCl_3$ solutions on a Bruker 500 MHz spectrometer. Predicted ^{1}H NMR chemical shifts were generated by using ACD/HNMR-2.5 software from Advanced Chemistry Development, Inc., Toronto, Canada. ^{13}C NMR spectra were run with both broad band proton decoupling and off resonance proton decoupling. The multiplicity observed in the off-resonance ^{13}C NMR spectra permits the determination of the number of protons bonded to each particular carbon.[34] Detailed listings of the NMR spectra for each of the compounds are given in the Supporting Information for this paper.

UV spectra of methylene chloride solutions were acquired on a Shimadzu UV-260 ultraviolet visible spectrometer. Fluorescence spectra were performed on a PTI fluorimeter. Spectra were obtained on methylene chloride solutions which had been degassed by bubbling argon through them for 10 min. Fluorescence quantum yields were determined using *N*-methylcarbazole as a reference. IR spectra of neat films on NaCl plates were recorded on a Perkin-Elmer Spectrum 2000 FT-IR spectrometer. High-resolution mass spectra were run at the University of California Riverside Mass Spectrometry Facility on a VG-ZAB instrument. Exact masses were determined by peak matching against known peaks of polypropylene glycol (795.5447 and 853.5865). Elemental analysis was carried out by Oneido Research Services, Whiteside, NY.

The glass transition temperature T_g and T_m of the tetramers were determined on a Perkin-Elmer DSC-7 instrument, calibrated with indium (melting point = 156 °C). The analysis program was 10 °C/min from 50 to 300 °C. TGA of the tetramers were measured on a Shimadzu TGA-50 instrument. The temperature was increased by 5 °C/min from 25 to 700 °C.

Tetraphenyl-tetraphenyethynyl-cyclooctratetraene, COT-H. Dihydridocarbonyltris(triphenylphosphine)ruthenium (55.1 mg, 60 μmol), toluene (3 mL), and styrene (6.8 μL, 60 μmol) were placed in an Ace pressure tube. The tube and its contents were purged with nitrogen for a few minutes. The tube was sealed and heated at 110 °C until the color of the catalyst solution had changed to orange. This color change indicates that the catalyst has been activated.[17] The tube and its contents

(32) Kijima, Y. Materials Research Society Abstracts, Spring Meeting, San Francisco, 1998. Baldo, M. A.; Lamansky, S.; Burrows, P. E.; Thompson, M. E.; Forrest, S. R. *Appl. Phys. Lett.* **1999**, *75*, 4. O'Brien, D. F.; Baldo, M. A.; Thompson, M. E.; Forrest, S. R. *Appl. Phys. Lett.* **1999**, *74*, 442.

(33) Levison, J. J.; Robinson, S. D. *J. Chem. Soc., A* **1970**, 2947.

(34) Günther, H. *NMR Spectroscopy*, 2nd ed.; J. Wiley & Sons: Chichester, England, 1995; pp 269−270.

were cooled to room temperature. The tube was opened under nitrogen and diphenylbutadiyne (404 mg, 2 mmol) was added. The solution was purged with nitrogen and the tube was sealed. The tube and its contents were heated at 135 °C overnight. The toluene solvent was removed by evaporation under reduced pressure. The residue was purified by column chromatography with silica gel and hexane/methylene chloride (4/1) as the eluent: yield, 0.35 g, 86%; mp 219−220 °C; by DSC T_g = 177 °C and T_m = 220 °C. NMR and IR: see Supporting Information. UV λ_{max} nm (ϵ): 365 (68000), 341 (44000), 313 (76000), 228 (44000). Fluorescence λ_{max} 392 nm in solution (quantum yield = 16%). MS: $M^{+\bullet}$ calcd for $(C_{16}H_{10})_4^+$: 808.3130, found 808.3159; the base peak corresponds to $(C_{16}H_{10})_3^+$. By TGA the tetramer is stable to 310 °C. Above 310 °C, a steady loss of weight occurs. By 650 °C, 98% of the initial sample weight is lost.

Tetra-*p*-tolyl-tetra-*p*-tolylethynyl-cyclooctratetraene, COT-Me. Dihydridocarbonyltris(triphenylphosphine) ruthenium (110 mg, 120 μmol), toluene (3 mL), and styrene (13.6 μL, 120 μmol) were placed in an Ace pressure tube. The catalyst was activated as above. Di-*p*-tolylbutadiyne (1.0 g, 1.1 mmol) was added, and the tube was purged with nitrogen and sealed. The tube and its contents were heated at 135 °C overnight. The product was purified by column chromatography (silica gel/hexane/ethyl acetate) to give a yellow solid (0.70 g): yield 70%, mp 263−265 °C, by DSC T_m = 265 °C and T_g = 214 °C. NMR and IR: see Supporting Information. UV λ_{max} nm (ϵ): 366 (49800), 317 (73000), 245 (32600). Fluorescence $\lambda_{\_max}$ 402 nm (quantum yield = 47%) when excited at 310−320 nm. The λ_{max} of the excitation spectrum is 375 nm. MS: $M^{+\bullet}$ calcd for $(C_{18}H_{14})_4^+$ 920.438, found 920.437. The base peak in the mass spectrum of **COT-Me** corresponds to $(C_{18}H_{14})_3^+$: calcd 690.3287, found 690.330. TGA: The tetramer is stable until 360 °C. From 360 to 600 °C, 97% of the initial sample weight is lost.

Tetra-*p*-anisolyl-tetra-*p*-anisolylethynyl-cyclooctatetraene, COT-OMe. Di-*p*-methoxyphenylbutadiyne was treated with activated ruthenium catalyst as above. After purification, the unsymmetrical cyclic tetramer was obtained in 29% yield: mp, 199−200 °C, by DSC T_g = 194 °C and T_m = 200 °C. NMR and IR: see Supporting Information. UV λ_{max} nm (ϵ) 365 (50000) 325−399 (65000). Fluorescence λ_{max} 412 nm (quantum yield = 79%) when excited at 310−320 nm. The λ_{max} of the excitation spectrum is 375 nm. The parent ion is not observed for this compound; however, the trimer fragment is observed as the base peak. Both **COT-Me** and **COT-H** showed very weak parent ions and the trimer as their base peaks. MS: $M^{+\bullet}$ calcd for $(C_{18}H_{14}O_2)_3^+$ 786.298, found 786.302. TGA: The tetramer is stable until 335 °C. From 335 to 566 °C, 94% of the initial sample weight is lost.

Tetra-2-thiophenyl-tetra-2-thiophenylylethynyl-cyclooctratetraene, COT-th. Ruthenium-catalyzed cyclotetramerization was carried out as above. In this way, 0.1 g of cyclic tetramer was obtained from 0.2 g of di-3′-thienylbutadiyne: mp 89−90 °C. NMR: see Supporting Information. CH analysis was satisfactory (calcd for $C_{48}H_{24}S_8$, C 67.25 and H 2.82; obsd, C 67.42 and H 2.93). By TGA, the tetramer is stable to 316 °C. Above 316 °C, a steady loss of weight occurs. By 635 °C, 98% of the initial sample weight is lost.

Preparation of Octaphenylcyclooctatetraene, C_8Ph_8. Lithium (0.26 g, 0.037 mol), which was carefully washed with ethanol and ether, was placed in a three-neck flask and purged with nitrogen three times. Diphenylacetylene (5 g, 0.028 mol) in 15 mL of ether solution was added to the above flask. The color changed to red-brown. After most of lithium metal had been consumed, this solution was transferred into an ether solution of iodine (2.45 g, 0.01 mol). The reaction color changes to yellow and the crude product precipitated from the solution. The mixture was filtered and the solid was extracted with THF for 3 h to remove the soluble byproducts. After recrystallization from diphenyl ether, 2.30 g (46% yield) of C_8Ph_8 was obtained. Melting point: 421−423 °C (lit[20] mp 425−427 °C).

Preparation of Tetraphenyl-tetra-*m*-tolyl-cyclooctatetraene, C_8Ph_4-(*m*-tol)$_4$. The procedure is the same as C_8Ph_8. In this way, 2.0 g of C_8Ph_4(m-tol)$_4$ was prepared from 3.6 g of phenyl-*m*-tolylacetylene (56%yield). This material is much more soluble than C_8Ph_8 in common organic solvents, e.g. methylene chloride, chloroform, etc. Mp 292−294 °C. NMR: see Supporting Information. MS, M^+: calcd for $(C_{15}H_{12})_4^+$ 768.3756, found 768.3764.

Molecular Modeling. Molecular modeling calculations were performed using the MacSpartan Plus, Version 1.19 (Wavefunction, Inc.) software package. All structures were optimized at the PM3 level of theory. Modeling was restricted to tetraphenyl-tetra(propynyl)-COT compounds because of software limitations. Alternate arrangements of the phenyl substituents or double bonds in the COT ring led to structures with similar tub-shaped geometries that varied <5 kcal/mol in energy.

OLED Fabrication and Testing. The devices were built on ITO coated substrate, which were cleaned by sequential ultrasonication in 1,1,1-trichloroethane, acetone, and 2-propanol, then dried in a stream of nitrogen. The samples (NPD, **COT-H**, **COT-Me**, perylene) were loaded onto the tantalum boats in the vacuum chamber, with a base pressure of 10^{-6} Torr. The deposition of materials was carried out by thermal evaporation from the boat at a deposition rate of 1−3 Å/s, as measured by a quartz crystal thickness monitor placed near the substrate. Electrodes consisting of Mg:Ag in a 10:1 atomic ratio were subsequently deposited on the whole sample by coevaporation from two separate Ta boats under a vacuum of 10^{-6} Torr. Without breaking the vacuum, a 1000 Å layer of Ag was then deposited to retard oxidation of the electrode.

The devices were characterized in air. Current−voltage measurements were made with a Keithley source meter (model 2400). Light intensity was measured using a Newport model 1835 optical power meter and silicon radiometer. EL spectra were measured with a Photon Technology International fluorimeter.

Acknowledgment. This work was supported by the Universal Display Corporation, the Defense Advanced Research Projects Agency, the National Science Foundation, and the Air Force Office of Scientific Research (MURI Program).

Supporting Information Available: Syntheses of the diarylalkyne and diaryldiyne starting materials, ^{1}H and ^{13}C NMR and IR spectral data for **COT-H**, **COT-Me**, **COT-OMe**, **COT-th**, and C_8Ph_4(*m*-tol)$_4$, absorption and emission spectra for **COT-Me**, **COT-th**, and C_8Ph_4(*m*-tol)$_4$, as well as the cyclic voltammograms of **COT-H**, **COT-Me**, and **COT-th**; the atom positions from molecular modeling study of C_8Ph_8 and tetraphenyltetraalkynyl-COT are also given (PDF). This material is available free of charge via the Internet at http://pubs.acs.org.

JA000354Q